# Monte Carlo simulation of cooperative orientation relaxation of dipoles in glass formers

C. Pareige,[1] H. Zapolsky,[1] and A. G. Khachaturyan[2]
[1]*Groupe de Physique des Matériaux, UMR 6634, Université de Rouen, Avenue de l'Universite BP 12 76801, Saint Etienne du Rouvray, France*
[2]*Department of Ceramics and Materials Science and Engineering, Rutgers University, 607 Taylor Road, Piscataway, New Jersey 08854, USA*
(Received 13 July 2006; revised manuscript received 14 November 2006; published 1 February 2007)

The glass transition in dipolar glass formers with long-range indirect dipole-dipole interactions has been studied by Monte Carlo simulation. Our simulation shows that the non-Arrhenien behavior of the relaxation time with temperature is induced by a progressive crossover from a regime of fast dynamics at high temperature in the polar liquid to one of slow dynamics controlled by the presence of polar clusters. The interaction between the clusters results in a spectrum of relaxation time and transition to the glass state. The glass transition starts at a temperature $T_0 > T_c$, below which spatial heterogeneities appear. These spatial heterogeneities start to influence the dynamical behavior and the spectrum of relaxation time becomes asymmetric. Below $T_c$, when the polar clusters reach a nanometric size ergodicity breaking occurs.

DOI: 10.1103/PhysRevB.75.054102 PACS number(s): 64.70.Pf, 77.22.Gm, 02.70.Uu, 77.84.−s

## I. INTRODUCTION

The glass transition phenomenon is one of the most exciting unsolved problems in the physics of condensed matter. It takes place when the viscosity upon cooling becomes so great that the molecular motion is arrested on the time scale of the experiment. This transition is often characterized by a temperature called $T_g$. For temperatures below $T_g$, the structure is like a disordered solid or a frozen liquid, the average relaxation time is very high and increases to reach a value of $10^2$ s at $T_g$.

Many recent experimental and computational studies of glass transition indicate the existence of "dynamic heterogeneity" and its major role in the glass transition of polymeric and other glass-forming liquids.[1–5] These deviations from "homogeneity" in the liquid dynamics are often accompanied by spatial dynamic heterogeneity induced by spatial correlation of particles in a state of enhanced or diminished mobility.[6,7] The structure of glasses has been studied extensively using spin-glass models.[8–11] These simulations predict a dynamic transition at a temperature $T_c$ below which ergodicity breaking occurs. The dynamic equations of these spin-glass models are similar to those of the mode-coupling theory (MCT) of liquids.[12] In the framework of MCT theory, nanometric heterogeneities appear at $T_c$ when the dynamics becomes cooperative.[13] The cooperative rearranging domains or regions are called CRR by Adam and Gibbs.[14] The cooperativity of the movements engaged in the vicinity of the glass transition is the most important characteristic of the associated relaxation process. At $T$ lower than $T_c$ the dynamics is dominated by activated processes. In the landscape scenario,[15,16] there exists a temperature $T_0 > T_c$ below which the energy landscape starts to influence the dynamical behavior.[17]

Another characteristic of the majority of glass formers during glass transition is a Vogel-Tammann-Fulcher (VTF)-type[18–20] temperature dependence for the relaxation time. This distinction is valid irrespective of the chemical structure of the liquid.

All these characteristics of glass transition are similar to the dielectric phase transition in relaxor ferroelectrics. The phase transition in relaxor ferroelectrics is a diffuse phase transition which can be attributed to the reorientation of some randomly oriented polar microregions originating from compositional fluctuations on the nanometer length scale. These chemical fluctuations result in the statistical distribution of the transition temperature and consequently the broad temperature dependence of dielectric properties. The relaxor behavior of these materials is attributed to these nanometer-size regions and to a thermally activated ensemble of superparaelectric clusters. The broad distribution of relaxation times for cluster orientations originates from the distribution of the potential barriers separating the different orientational states. A short-range cooperative interaction between these superparaelectric clusters was considered by Viehland *et al.*[21] to explain the freezing of the superparaelectric moments into a dipolar glass with a ferroelectric order at lower temperatures. The freezing of dielectric relaxation in relaxor ferroelectrics was directly evidenced by Gazounov and Tagantsev[22] following the VTF law.

Recently the aspect of dipole relaxation in ferroelectric materials has been investigated by Su *et al.*[23,24] They have proposed a Ginzburg-Landau coarse-grain-type theory employed for Monte Carlo simulation of the dielectric properties of relaxor ferroelectric materials. Using the resemblance between the dielectric phase transition in the relaxor ferroelectrics and the glass transition in glass formers, in this paper we apply the model first proposed by Vugmeister[25] with recent developments by Su *et al.*[23] This model successfully reproduces the dielectric properties of relaxors and is used to describe the dynamics in a polar glass former whose molecular group has a dipole flip moment. This polar system is regarded as an ensemble of randomly distributed rotating local dipoles coupled by strong long-range indirect dipole-dipole interaction. The dielectric response of the system to the applied electric field thus consists of two effects, the polarization of the molecules of the glass, which does not include the effect caused by the dipole rotation, and the polarization caused by a rotation of local dipole moments par-

 ©2007 The American Physical Society

tially hindered by the long-range indirect dipole-dipole interaction. In this study we will focus on the latter effect. It will be shown that the long-range interaction of randomly distributed rotating electric dipoles significantly modifies the dielectric response and the VTF law of the relaxation time, resulting in the collective freezing of the dipole rotation and the appearance of polar clusters.

This paper is organized as follows: in Sec. II, we review the equations governing our model; in Sec. III, we present the numerical scheme; in Sec. IV, we discuss our numerical results in comparison with previous models; and in Sec. V, we give conclusions and describe work in progress.

## II. MODEL

We consider three-dimensional highly polarizable systems with cubic symmetry where a number of dipoles are distributed randomly. The interaction between dipoles arises from the fact that each dipole polarizes the lattice, and this dipole-induced polarization acts on the adjacent dipole. As a result, the "indirect" dipole-dipole Hamiltonian interaction is

$$H = -\frac{\gamma^2}{2} \sum_{\substack{s,s' \\ s \neq s'}} \mathbf{d}_i(\mathbf{r}_s) J_{ij}(\mathbf{r}_s - \mathbf{r}_{s'}) \mathbf{d}_j(\mathbf{r}_{s'}), \tag{1}$$

where $\gamma$ is the coupling constant between a local dipole and the host lattice polarization (its magnitude is of the order of the Lorentz constant $4\pi/3$), $\mathbf{d}(\mathbf{r}_s)$ is the effective dipole moment of the $s$th local dipole, the index $s$ numbers all local dipoles ($s=1,2,\ldots,N_d$), $J_{ij}(\mathbf{r}_s-\mathbf{r}_{s'})$ is the interaction energy between two dipoles situated at sites $\mathbf{r}_s$ and $\mathbf{r}_{s'}$. In our model, the interaction energy is associated with the electrostatic interaction of the polar clusters in the host lattice can be written in the following form:[23]

$$J(r)_{ij} = \frac{1}{4\pi\alpha^{-1} r_{\mathrm{corr}}^3} \left[ \frac{\exp(-\rho)}{\rho} \delta_{ij} + \left( \delta_{ij} - 3\frac{\rho_i \rho_j}{\rho^2} \right) \times \left( -\frac{1}{\rho^3} + \frac{\exp(-\rho)}{\rho^3} + \frac{\exp(-\rho)}{\rho^2} \right) - \frac{\rho_i \rho_j}{\rho^3} \exp(-\rho) \right], \tag{2}$$

where $\rho = r/r_{\mathrm{corr}}$ is the norm of the vector $\boldsymbol{\rho}$, $\alpha$ is the susceptibility of the media, $r_{\mathrm{corr}}$ is the correlation length ($r_{\mathrm{corr}} = \sqrt{\beta\alpha}$ where $\beta$ is a material constant). The correlation length is a material constant at a given temperature that characterizes the typical size of the polar cluster generated by a local dipole. It is interesting to note that if $\alpha \to \infty$, the asymptotic behavior of the function $J_{ij}(\mathbf{r})$ is proportional to $1/r$. This attractive interaction is thus much stronger and more long-ranging than the direct dipole-dipole interaction which decays as $1/r^3$. This indicates that indirect dipole-dipole interaction increases the cooperative effect and can cause the freezing of the dipole clusters into a dipolar glassy state. The strength of this interaction is governed by the value $r_{\mathrm{corr}}$ and can be related to the fragility of glass forming liquids. It is a well-recognized fact that network-forming covalent liquids, with very strong interaction between the molecules, are also strong glass formers. Thus choosing the $r_{\mathrm{corr}}$ value we can reproduce different classes of glass forming liquids.

For the convenience of numerical calculation, Eq. (1) is transformed into a dimensionless form through the introduction of a reduced energy defined as

$$H^* = H \Big/ \left( \frac{\gamma^2 d_0^2}{4\pi\alpha^{-1} r_{\mathrm{corr}}^3} \right), \tag{3}$$

where $d_0$ is the norm of the dipole moment at 0 K. Let us introduce the following reduced variables: $\boldsymbol{\eta}(\boldsymbol{\rho}_s) = \mathbf{d}(\boldsymbol{\rho}_s)/d_0$ is the reduced dipole moment of the dipole at site $s$, $\boldsymbol{\rho}_s = \mathbf{r}_s / r_{\mathrm{corr}}$ is position, and $\Phi(\boldsymbol{\rho}_s - \boldsymbol{\rho}_{s'})$ is the dimensionless form of $J_{ij}(r_s - r_{s'})$. The dimensionless form of interaction Hamiltonian is

$$H^* = -\frac{1}{2} \sum_{\substack{s,s' \\ s \neq s'}} \eta(\rho_s)_i \Phi(\rho_s - \rho_{s'}) \eta(\rho_{s'})_j. \tag{4}$$

As was discussed in Ref. 23, it is convenient to use the parameter $n_d$ to characterize the dependence of the thermodynamics and kinetics of the system on a given interaction Hamiltonian. The reduced parameter $n_d$ is defined as

$$n_d = \frac{4\pi}{3} r_{\mathrm{corr}}^3 c, \tag{5}$$

where $c$ is the concentration of dipoles. The parameter $n_d$ is the average number of local dipoles interacting with the selected dipole (or the average number of dipoles located within a sphere of the correlation radius $r_{\mathrm{corr}}$ around the selected dipole). Consequently, different correlation lengths $r_{\mathrm{corr}}$ and concentrations $c$ should give the same results, as long as they provide the same value of $n_{\mathrm{d}}$.

With these definitions of variables, the partition sum of the system is

$$Z = \sum e^{(-H^*_{conf}/T^*)}, \tag{6}$$

where the summation is taken over all possible configurations and corresponds to all possible directions of local dipoles, and

$$T^* = k_B T \Big/ \left( \frac{\gamma^2 d_0^2}{4\pi\alpha^{-1} r_{\mathrm{corr}}^3} \right) \tag{7}$$

is the reduced temperature, $k_{\mathrm{B}}$ being the Boltzmann constant. Therefore the total reduced energy of the system is a function of the two dimensionless parameters $T^*$ and $n_{\mathrm{d}}$.

## III. MONTE CARLO SIMULATION

Monte Carlo simulation is performed on a three-dimensional (3D) $L=128$ lattice with periodic boundary conditions. 21 000 dipoles are distributed over $128^3$ sites of the system (the concentration of dipoles is $c=1\%$). The correlation length is taken equal to $4a$. This corresponds to $n_{\mathrm{d}} = 2.68$, meaning that if we select any dipole, an average of 2.68 dipoles interact with it. It is assumed that each dipole is allowed to take only six different orientations: $[\pm 1,0,0]$, $[0,\pm 1,0]$, and $[0,0,\pm 1]$. The change of the configuration

corresponds to a dipole flip from one state to another at site $i$. Assuming that the thermally activated dipole flip is the unique mechanism involved in changing the configuration, we perform the simulation via the Metropolis algorithm. The flip is accepted with the probability $W$:

$$W = \begin{cases} 1 & \text{if } \Delta H^* \leq 0 \\ \exp\left(-\dfrac{\Delta H^*}{T^*}\right) & \text{if } \Delta H^* > 0, \end{cases} \tag{8}$$

where $\Delta H^*$ is the change on the Hamiltonian [Eq. (3)] caused by a tested flip. Since all dipoles are randomly distributed and are in different orientation states, each dipole has a different environment. This results in a situation where each dipole, in general, has a different potential because this potential is generated by differently located neighboring dipoles in different configurations.

The screened indirect dipole-dipole interaction potential, Eq. (2), was cut off at $10a$, where $a$ is the cubic lattice parameter. We compared our calculations, which were performed in real space with $r_{\text{cutoff}}$, with the previous calculations for a similar system using the Debye approximation,[23] and both models gave the same results. Recently, it has been demonstrated[26,27] that in the case of dipole-dipole interaction, $\Delta H^*$ becomes almost independent of $r_{\text{cutoff}}$ if $r_{\text{cutoff}} > 6a$. We also tested the influence of the size effect of the simulation box on the final state of the system. We will discuss this point below.

Similarly to the thermally stimulated current experiments, the initial configuration for each Monte Carlo (MC) simulation is assumed to be fully ordered, i.e., all the dipoles have the same orientation (one of the six possible orientations). Thus the macroscopic polarization in this state assumes the maximum value. This nonequilibrium state is placed at the reduced temperature $T^*$ and relaxes by MC simulation. To investigate the changes of the value of the macroscopic polarization with temperature, the macroscopic polarization at temperature $T^*$ is measured by spatial averaging over all dipoles and temporal averaging over a large number of Monte Carlo steps:

$$\bar{\eta} = \frac{\sum_s \langle \eta(\rho_s) \rangle}{N_d}, \tag{9}$$

where $\langle \eta(\rho_s) \rangle$ is the average value of polarization of the $s$th dipole over the observation "time." The averaging is done after MC equilibration has been reached. The value of macroscopic polarization at a given temperature has been averaged over 16 different simulations.

To test the ergodicity of simulated system, we also started our calculations from a completely disordered state. As we will show below, MC simulations show that under some temperatures the final state becomes history dependent and thus the system ceases to be ergodic.

One of the most important characteristics of glass transition is the relaxation time. It is determined as follows: for the $s$th dipole, the relaxation time $\tau_s$ corresponds to the time it needs to overcome the energy barrier $E(s)$ in order to flip. The interaction of the dipole with its neighbors changes $E(s)$. Making the usual assumption that this change is equal to half of the change of the interaction energy $\Delta H(s)$ produced by the tested flip,

$$E(s) = E_0 + \tfrac{1}{2}\Delta H(s),$$

where $E_0$ is the energy barrier in a dilute system in the absence of any interaction with neighboring dipoles.

Under these assumptions, the relaxation time $\tau_s$ is

$$\tau_s = \tau_{00} \exp\left(\frac{E(s)}{k_B T}\right) = \tau_0 \exp\left(\frac{\Delta H(s)}{2k_B T}\right), \tag{10}$$

where $\tau_{00}$ is the pre-exponential factor and $\tau_0 = \tau_{00} \exp\left(\frac{E_0}{k_B T}\right)$ is the typical relaxation time in a dilute system.

Because the value of $\Delta H(s)$ is different for each tested flip, the relaxation times form a spectrum. The test of $M_0$ elementary flips produces a spectrum of $M_0$ values of $\xi = \tau_s/\tau_0 = \exp(\Delta H^*/2T^*)$. The spectrum of relaxation times is characterized by the frequency histogram $P(\xi)$ that determines the relative number $\Delta M(\xi)/M_0$ of relaxation times within the range $(\xi, \xi+\Delta\xi)$.

The spectrum of relaxation times results from the frequency dispersion of the susceptibility $\chi(\omega)$. The real and imaginary parts of $\chi(\omega)$ are given by

$$\chi'(\omega) = \chi(0)\frac{1}{M_0}\sum_{s=0}^{M_0} \frac{1}{1+[\omega\tau_0 \exp(\Delta H_s/2k_B T)]^2} = \chi(0)\int_{\xi=0}^{\infty} \frac{1}{1+[\omega\tau_0\xi]^2} Q(\xi)d\xi, \tag{11}$$

$$\chi''(\omega) = \chi(0)\frac{1}{M_0}\sum_{s=0}^{M_0} \frac{\omega\tau_0 \exp(\Delta H_s/2k_B T)}{1+[\omega\tau_0 \exp(\Delta H_s/2k_B T)]^2} = \chi(0)\int_{\xi=0}^{\infty} \frac{\omega\tau_0\xi}{1+[\omega\tau_0\xi]^2} Q(\xi)d\xi, \tag{12}$$

where $Q(\xi)$ is deduced from $P(\xi)$ as follows: $Q(\xi) = \frac{1}{\Delta\xi}P(\xi)$, $\omega$ is the frequency of the applied field, and $\chi(0)$ is the static susceptibility of the entire system.

The output is curves of $\chi''/\chi(0) = f(\omega/\omega_0)$ and $\chi'/\chi(0) = f(\omega/\omega_0)$ at reduced temperature $T^*$. The maximum of the loss factor $\chi''/\chi(0)$ corresponds to the value of the relaxation time $\tau/\tau_0$ at temperature $T^*$.

## IV. RESULTS AND DISCUSSION

Figure 1 shows the simulated dependence of the reduced macroscopic polarization of the system vs the reduced temperature $T^*$ obtained by the equilibration of the poled or of the disordered initial state.

The MC equilibrations were carried out without an applied electric field, so the spontaneous relaxation of the fully ordered state results in a completely disordered state at high temperature leading to a vanishing value for the macroscopic polarization. When the temperature decreases, the thermal energy becomes too low to completely relax the fully or-

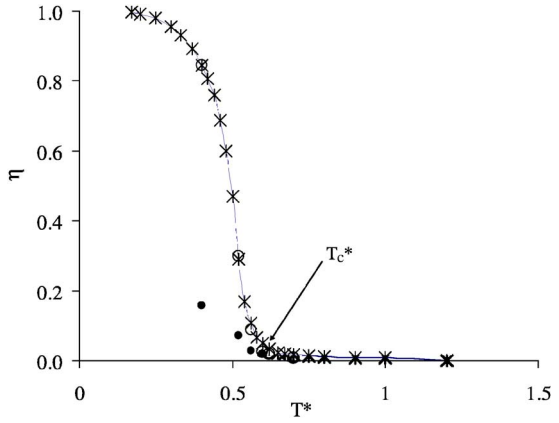


FIG. 1. (Color online) Simulated dependence of the reduced macroscopic polarization $\eta$ on the temperature $T^*$ with no electric field. The crosses determining the curve are the simulated points obtained by isothermal equilibration of the fully ordered state in a simulation box of size 128. Each cross corresponds to an averaged value over 16 different simulations. The open circle corresponds to the measurements in the case of a simulation box of size 200. The curve formed by the dots is obtained by isothermal equilibration of the disordered initial state in a simulation box of size 200. $T_c^*$ marks the temperature where the system becomes nonergodic.

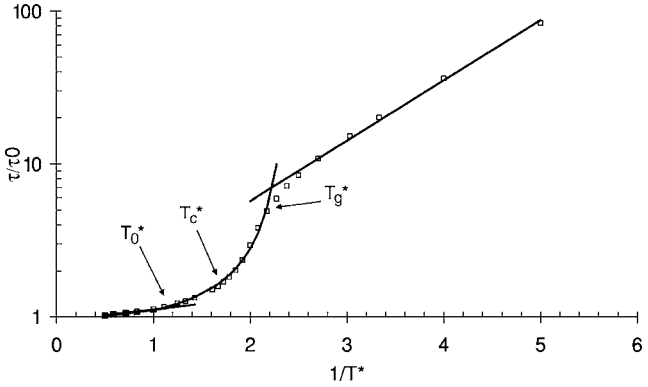


FIG. 2. Simulated dependence of the relaxation time on the inverse of $T^*$. The VTF behavior is clearly observed. Non-Arrhenius behavior of relaxation time with temperature starts at $T_0^*$. $T_c^*$ indicates the temperature where the system becomes nonergodic. At $T_c^* < T < T_g^*$ a certain number of dipoles are frozen in the initial configuration. For temperature $T^* < T_g^*$ the dynamics is controlled by the slow process.

dered state, thus leading to a macroscopic polarization. In the case of thermal equilibration of the initially disordered state a vanishing value for polarization is expected at low temperature. Nevertheless, a small polarization is measured (Fig. 1). To understand this observation we studied the value of macroscopic polarization at low temperature for different sizes of simulation boxes. As expected, it was observed that the value of $\bar{\eta}$ is very sensitive to the ratio of $r_{\mathrm{corr}}/L$. At low temperature, we found that for $L=128$, the value of $\bar{\eta}$ tends towards the value obtained for the initially ordered state. There is a strong indication that the small remaining polarization is an artifact caused by the size of the simulation box (see Fig. 1 for $L=200$), and by the fact that the measurements are carried out for a finite time, whereas there is a significant slowing down of the relaxation kinetics near the $T_g$ temperature.

It should be possible to obtain a vanishing value for the polarization with a greater value of $L$ and a longer simulation time. Figure 1 shows that there is a minor influence of $L$ (between the values 128 and 200) on the final state after the thermal equilibration of the fully ordered state. Our simulations were thus carried out with $L=128$.

From Fig. 1, it follows that at temperatures below $T_c=0.6$ the final state of the system gradually becomes history dependent and thus the system becomes nonergodic. This temperature has the same significance as the critical temperature in MCT theory.

This diffuse ferroelectric transition appears at the value of $n_d \sim 1$. Therefore we have here three different ranges, $n_d \ll 1$, $n_d \gg 1$, and $n_d \sim 1$:

(i) At small concentration of dipoles ($n_d \ll 1$), the system can be described as a dilute state where each dipole is independent. In this case the $r_{\mathrm{corr}}$ is smaller than the mean distance between the dipoles.

(ii) At high concentration of dipoles ($n_d \gg 1$), the system is described by the mean-field approximation—it no longer "feels" the individual dipoles and behaves as a homogeneous material with a "normal" ferroelectric transition. The results of the recent paper by Zhang and Widom[28,29] are in agreement with this scenario. This paper showed that the frozen amorphous dipolar systems described by the mean-field theory could also have a spontaneous ferroelectric order for a density of dipoles $\rho > \rho_c$. Monte Carlo and molecular-dynamics simulations also confirm the influence of the initial concentration of dipoles on the nature of the transition from the liquid phase.[30,31]

(iii) The most interesting case considered in this paper is $n_d \sim 1$. This is the only case where a dipolar glass phase can appear and the ferroelectric transition becomes diffuse. The relaxor ferroelectric behavior was observed in the poly(vinylidene fluoride-trifluoroethylene) copolymer system which is a glass former system.[32]

Using the imaginary part of susceptibility, we calculated the relaxation time at a given temperature (Fig. 2). The simulated dependence of the relaxation time with $1/T^*$ is in very good agreement with experimental curves. One of the reasons for the small number of decades on simulated curves can be related to the fact that in our simulations we do not take into account the temperature dependence of the correlation radius $r_{\mathrm{corr}}$. Figure 2 shows that at high temperature an Arrhenius behavior is observed up to $T_0^*=0.9$; this marks the beginning of a non-Arrhenien behavior, which can be fitted to the VTF law. At very low temperatures (under $T^* \sim 0.4$), the behavior of the relaxation time with $1/T^*$ can also be describe by an Arrhenius law. Even though the glass transition temperature is a kinetic notion (and, in this work, the kinetics is not simulated), we can suppose that $T_g^*$ lies in the temperature range where the VTF behavior and the Arrhenius behavior at low temperature are no longer observed (between $T^*=0.46$ and $T^*=0.4$). If we define the temperature $T_g^*$ as a temperature below which relaxation time vs $1/T^*$ ceases to be described by a VTF law, then we can conclude that $T_g^* \approx 0.46$.

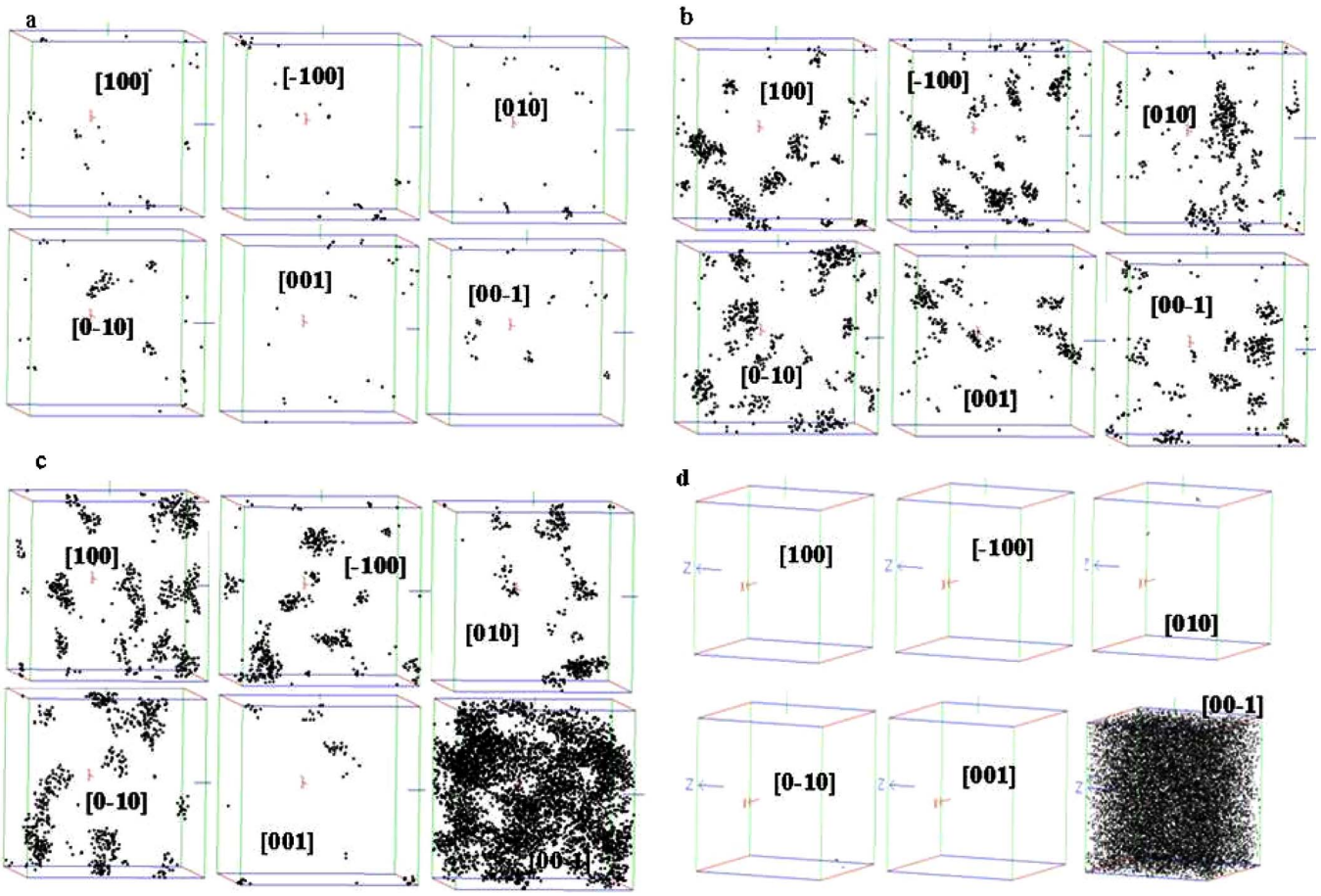


FIG. 3. (Color online) 3D images of the distribution of the dipoles within polar domains defined as clusters of dipoles in the six possible orientations. Only areas where at least 60% of the dipoles are in the same orientation are visualized. Thus all the dipoles are not represented. The initial orientation of the dipoles was (00−1). (a) $T^*=0.8$; (b) $T^*=0.6$; (c) $T^*=0.52$; (d) $T^*=0.33$.

The numerous experimental data[12,33,34] show that $T_c \sim 1.2T_g$. Our numerical results are in good agreement with this observation ($T_c^* \sim 1.25T_g^*$). It can be noted that no change in the behavior of the relaxation time with $1/T^*$ is observed at $T_c^*$.

To relate the behavior of the polarization and the relaxation time to the spatial heterogeneities in the system, we studied the 3D distribution of the dipoles. The 3D images presented in Fig. 3 show the 3D distribution of the dipoles and their orientation in the simulated volume at temperature $T^*$ equal to 0.8 ($T_c^*, < T^* < T_0^*$), to $T_c^*=0.6$, to 0.52 ($T^* < T_c^*$) and to $T^*=0.33 (T^* < T_g^*)$. Not all the dipoles are represented on these images. Only areas where at least 60% of the dipoles are in the same orientation are visualized. These images clearly show the existence of heterogeneities that form polar clusters. The size of the domains becomes higher as the temperature decreases. An analysis of the simulated images at each temperature indicates that the polar domains appear for temperatures below $T_0^*=0.9$. Below $T_c^*$, the size of the polar domain increases markedly. The more the temperature decreases, the more the domains in the initial orientation in $[00\bar{1}]$ are prominent (Fig. 3) and at $T^* < T_g^*$, most of the dipoles are frozen in the initial configuration. The phenomenon of heterogeneity at the nanometric scale above $T_c$ is observed experimentally and predicted by simulation.[35,36] In our approach this phenomenon appears naturally. These polar clusters can be associated with regions of cooperative rearrangement. All the dipoles in the clusters rotate together as a "rigid" unit. To provide this rotation, the system needs much more time than for a rotation of one isolated dipole and thus becomes dynamically heterogeneous. The slow and fast rotation dynamics coexist at the same time, as is shown in Fig. 4 and they are linked to the existence of spatial heterogeneities in the system.

The appearance of heterogeneities produces a broadening of the distribution of relaxation times as is shown by the frequency histograms of the relaxation time (Fig. 4). In our model, a typical relaxation time is strongly temperature dependent and is determined by Eq. (10). The activation barriers for dipole flip depend on interaction of a local dipole with other dipoles. This interaction occurs through polarization of the host lattice. In the general case, if this interaction is absent (a dilute system, $n_d \ll 1$), the typical relaxation process for each local dipole and its clusters is determined by a single relaxation time $\tau_0$. In our case ($n_d=2.38$) where the correlation radius $r_{corr}$ is commensurate with the average distance between local dipoles $r_d$, the interaction between local dipoles becomes large enough to split the single relaxation time $\tau_0$ into a spectrum of relaxation times $\tau$.

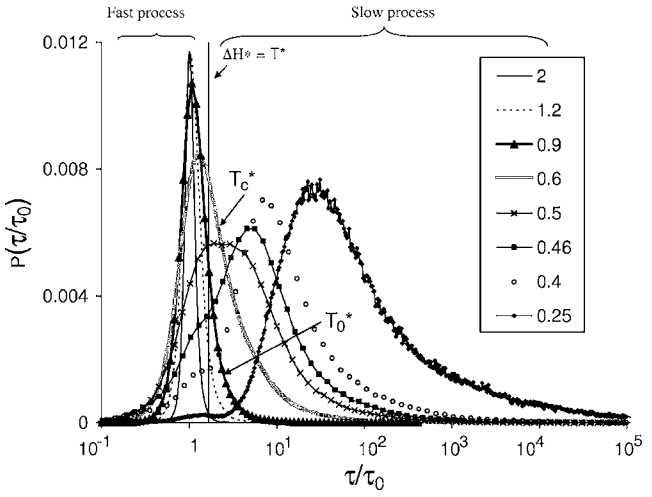


FIG. 4. Frequency distribution of relaxation times for different temperatures. The vertical line corresponds to the value $\Delta H^*=T^*$. $T_c^*$ marks the appearance of a shoulder in the distribution of relaxation times. For $T_g^*<T^*<T_0^*$ slow and fast dynamics coexist. Under $T_g^*$ the dynamics is controlled by slow processes.

The vertical line (see Fig. 4) corresponds to the value of $\Delta H^*=T^*$. At high temperature, the greater part of the relaxation time distribution is on the left of the vertical line. The great majority of the flips are nonthermally activated (the energy barrier $\Delta H^*$ is lower than thermal agitation). Moreover, the mean of the distributions varies slowly with the temperature, the macroscopic polarization vanishes (Fig. 1), and no polar clusters are observed: this corresponds to a liquidlike state. When the temperature decreases, the jumps from one configuration to another start to be thermally activated: a slow dynamics appears which is associated with the appearance of the spatial heterogeneities (polar clusters): below $T_0^*$, the large time tail of the distribution develops. Our interpretation of $T_0^*$ is in excellent agreement with the $T_0$ defined in landscape theory.[17] This theory predicts that the relaxation involves only a fast process at high temperature. At $T>T_0$, the dynamics is governed by nonbarrier diffusion because the activation barriers are small in height: below $T_0$, the local minima of the potential energy start to decrease and the potential-energy landscape starts to influence the dynamic behavior.[35] Under $T_c$, we clearly observe the two maxima which correspond to a mixed regime where both fast and slow processes coexist. There is a progressive crossover from a regime of fast dynamics at high temperature in the polar liquid to one of slow dynamics which is controlled by the polar cluster. With decreasing of temperature, slow processes become dominant. The displacement of the maximum of the peak for the slow processes is the signature of the increase in size of the polar cluster. When the system is almost frozen, the high-frequency maximum of the relaxation time distribution function disappears. In a landscape scenario, at low temperature the dynamics in the system is also controlled by over-barrier jumps, which result from the increasing height of the acting barriers.

The simulated dependence on temperature of the shape of the relaxation time distribution, shown in Fig. 4, is in very good agreement with experimental curves obtained in glassy freezing of a deuteron dipole glass.[36] Berthier *et al.*[37] observe similar frequency distributions of relaxation times by Monte Carlo simulation. They have used a coarse grained approach which takes into account the dynamics heterogeneities. The basis of their work relies on two observations: (i) at low temperature, very few particles are mobile, (ii) when the macroscopic region of space is mobile, it influences the dynamics of neighboring regions, enabling them to become mobile too. This is the concept of dynamic facilitation.[38,39] In the work of Berthier *et al.*, $T_c^*$ is the temperature at which the fast process disappears. In our work, $T_c^*$ does not have the same meaning. It marks the temperature of loss of ergodicity. At $T_c^*$, the fast process is always the main process observed. When the fast process disappears, the system is in a glassy polar state. This is confirmed by the simulated dependence of the relaxation time on the inverse of temperature $T^*$ shown in Fig. 2. For the temperature range corresponding to the crossover regime, a VTF behavior is clearly observed up to $T^*=0.46$. These results clearly show that the non-Arrhenius behavior of the relaxation time is induced by the coexistence of both slow and fast dynamics, which is a consequence of spatial heterogeneity. Arrhenius law is observed when only a fast (or slow) process is observed. Under $T_g^*=0.46$, the frequency distribution of relaxation times shows a majority of slow processes. In other words, the glass transition is observed when the slow dynamics dominates.

The results obtained for this specific model of randomly located flipping dipoles with the long-range screened dipolar interaction seems to be a prototype for a wide class of random systems such as systems with deviation from stoichiometry, the randomly distributed atoms, or static defects.[40–42]

A common feature producing the spin-glass behavior in any system is the presence of spatially static randomly distributed defects that are dynamically orientated, the dilution of these defects being such that the average distance between the defects is of the order of an effective interaction radius.

The spin-glass behavior should be observed in systems if (i) the dynamic equations of motion of different particles are randomly different, but time-invariant (i.e., dynamic equations such as Newton or other mechanical equations of motion do not explicitly depend on time, and (ii) the distinction between the parameters of the dynamic equations for different particles is significant (the potential-energy barrier is commensurate with the heat energy $kT$).

Condition (i) is satisfied in our model because the potential barrier for the mechanical motion of each particle is *static* and *different* for each particle. Condition (ii) is satisfied if the distance between particles is commensurate with their interaction radius, $n_d \sim 1$. Otherwise, if the distance between particles is much greater than the interaction radius ($n_d \ll 1$, diluted system) the potential energy of the equation of motion is static but the same for all particles. Thus the system is conventional: it is ergodic and is described by the Gibbs thermodynamics.

If the distance between the particles is much smaller than the interaction radius ($n_d \gg 1$, concentrated system), then the particle interacts with many neighboring particles within the interaction radius sphere and thus interacts with the well-averaged (mean-field) potential produced by all these neighbors. The greater the number of these neighboring particles

around a test particle, the smaller the relative difference between this potential and potentials acting on other test particles. In other words, in the $n_d \gg 1$ case, the average *static* deviations from the same average potential acting on each defect is small and can be neglected. This is a situation described by the mean-field approximation for the potential. Then, when the potential (dynamic equation of motion) for each particle is the same, the particles are again described by the ergodic Gibbsian thermodynamics.

In the case of $n_d \sim 1$ alone, the difference between the neighbor-generated potentials acting on each particle is of the same order as the average potential and the entire statistical thermodynamics becomes non-Gibbsian and nonergodic. This is the spin-glass case.

All these systems show the same features, viz. a diffuse character of phase transition from high to low temperature, spatial and dynamic heterogeneities in the crossover region, and a kinetics slowdown.

## V. CONCLUSION

In this paper, we have studied the diffuse ferroelectric transition in a dipolar system that was simulated by randomly distributed dipoles coupled with strong long-range indirect dipole-dipole interactions. We have focused on the temperature dependence of macroscopic polarization as well as on the relaxation behavior of the system. Both initially ordered and disordered configurations of dipoles were considered. When the temperature decreases, three different regimes have been observed. At high temperature, the dynamics is liquidlike. The relaxation process is fast and no spatial heterogeneities are observed. All the dipoles are free to rotate. An Arrhenius behavior of the relaxation time is observed. Under $T_0^*$, small polar regions are nucleated. This leads to the appearance of the slow dynamics. A certain number of jumps from one configuration to another become thermally activated. The height of some activated barriers is larger than the thermal energy. This temperature $T_0^*$ can be compared to the temperature $T_0$ of the landscape. The nucleation of heterogeneities does not induce a loss of ergodicity, but markedly influences the behavior of the relaxation time: a VTF law is observed.

Under $T_c^*$, the system loses its ergodicity. This corresponds to the definition of $T_C$ given by MCT and by landscape. With decreasing temperature, the clusters become bigger and slow dynamics becomes more and more dominant. From $T^* < T_c^*$, the thermal energy becomes insufficient to overcome most of the energy barriers. A certain number of dipoles are frozen in the initial configuration. Around $T_g^*$, the slow process dominates.

The VTF behavior observed for $T_g^* < T^* < T_0^*$ is directly related to the mixed dynamics. For temperature $T^* < T_g^*$ the dynamics is controlled by the slow process.

In our model the relaxation time distribution appears naturally from the distribution of activation barriers for dipoles in the system studied. At high temperature, where fast processes are dominant, the distribution is Gaussian. With decreasing of temperature, there are two peaks in the distribution, reflecting the coexistence of polar clusters with a liquidlike state. This model relates the microscopical structure of the glassy state with the macroscopical behavior of the system. Computer simulations explain the origin of the diffuse nature of the glass transition. The reduced total polarization $\eta$ per site gradually vanishes by asymptotically approaching zero. It can be interpreted as a "diffuse" phase transition typical of a spin-glass transition.

Finally, it is worth noting that indirect dipole-dipole interactions in the polar media can explain the most important characteristics of glass transition in the dipolar amorphous state. The strength of this interaction is controlled by $r_{corr}$ which is a key physical factor controlling the fragility. This model is generic and has been used to describe the phenomenology of a wide variety of systems.

Finally, we note that the present paper has focused on the qualitative description of glass transition, rather than on reproducing real relaxation curves. In principle, this model could be extended to yield a quantitative description of glass transition. However, this would require introducing some models to describe the evolution of the activation barrier with the temperature and the temperature dependence of static susceptibility ($r_{corr}$), which is not yet known for the dipolar glass systems.

## ACKNOWLEDGMENTS

This work was supported by the computer-time Grant No. 2014006 of the Centre de Ressources Informatiques de Haute Normandie (CRIHAN). The financial support of NSF Grant No. DMR-0242619 for A.G.K. is gratefully acknowledged. We wish to thank J-M. Saiter for fruitful discussions and Dilys Moscato for her precious help and for carefully reading the manuscript.

[1] M. D. Ediger, Annu. Rev. Phys. Chem. **51**, 99 (2000).
[2] K. Binder, J. Baschnagel, and W. Paul, Prog. Polym. Sci. **28**, 115 (2003).
[3] L. Berthier and J. P. Garrahan, Phys. Rev. E **68**, 041201 (2003).
[4] M. D. Ediger, C. A. Angell, and S. R. Nagel, J. Phys. Chem. **100**, 13200 (1996).
[5] E. Bertin, J.-Ph. Bouchaud, and F. Lequeux, Phys. Rev. Lett. **95**, 015702 (2005).
[6] U. Tracht, M. Wilhelm, A. Heuer, H. Feng, K. Schmidt-Rohr, and H. W. Spiess, Phys. Rev. Lett. **81**, 2727 (1998).
[7] E. Vidal-Russel and N. E. Asraeloff, Nature (London) **408**, 695 (2000).
[8] T. R. Kirkpatrick and P. G. Wolynes, Phys. Rev. B **36**, 8552 (1987).
[9] G. Parisi, M. Picco, and F. Ritort, Phys. Rev. E **60**, 58 (1999).
[10] M. A. Moore and B. Drossel, Phys. Rev. Lett. **89**, 217202 (2002).

[11] M. A. Moore and J. Yeo, Phys. Rev. Lett. **96**, 095701 (2006).
[12] W. Götze and L. Sjörgen, Rep. Prog. Phys. **55**, 241 (1992).
[13] C. A. Angell, J. Phys. Chem. Solids **49**, 863 (1988).
[14] G. Adam and J. H. Gibbs, J. Chem. Phys. **43**, 139 (1965).
[15] J. H. Gibbs, in *Modern Aspects of the Vitreous State*, edited by J. D. McKenzie (Butterworths, London, 1960).
[16] M. Goldstein, J. Chem. Phys. **51**, 3728 (1969).
[17] S. Sastry, P. G. Debenedetti, and F. H. Stillinger, Nature (London) **393**, 554 (1998).
[18] G. S. Fulcher, J. Am. Ceram. Soc. **8**, 339 (1923).
[19] G. Tammann and W. Hesse, Z. Anorg. Allg. Chem. **156**, 245 (1926).
[20] H. Vogel, Phys. Z. **22**, 645 (1921).
[21] D. Viehland, J. F. Li, S. J. Jang, L. E. Cross, and M. Wuttig, Phys. Rev. B **46**, 8013 (1992).
[22] A. E. Glazounov and A. K. Tagantsev, Appl. Phys. Lett. **73**, 856 (1998).
[23] C.-C Su, B. Vugmeister, and A. G. Khachaturyan, J. Appl. Phys. **90**, 6345 (2001).
[24] C.-C Su, Ph.D. thesis, Rutgers University, 2001.
[25] B. E. Vugmeister and M. D. Glinchuk, Rev. Mod. Phys. **62**, 993 (1990).
[26] S. Fazekas, J. Kertész, and D. E. Wolf, Phys. Rev. E **68**, 041102 (2003).
[27] C. Eisenmann, U. Gasser, P. Keim, G. Maret, and H. H. von Grunberg, Phys. Rev. Lett. **95**, 185502 (2003).
[28] H. Zhang and M. Widom, J. Magn. Magn. Mater. **122**, 119 (1993).
[29] H. Zhang and M. Widom, Phys. Rev. B **51**, 8951 (1995).
[30] D. Wei and G. N. Patey, Phys. Rev. Lett. **68**, 2043 (1992); Phys. Rev. A **46**, 7783 (1992).
[31] J. J. Weis, D. Levesque, and G. J. Zarragoicoechea, Phys. Rev. Lett. **69**, 913 (1992).
[32] S. Ikeda, H. Suzuki, and S. Nagami, Jpn. J. Appl. Phys., Part 1 Part 1 **31**, 1112 (1992).
[33] H. Sillescu, J. Non-Cryst. Solids **243**, 81 (1999).
[34] E. Leutheusser, Phys. Rev. A **29**, 2765 (1984).
[35] F. H. Stillinger and T. A. Weber, Phys. Rev. A **25**, 978 (1982); **28**, 2408 (1983); Science **255**, 983 (1984).
[36] Y.-S. Choi and J.-J. Kim, Europhys. Lett. **65**, 55 (2004).
[37] L. Berthier and J. P. Garrahan, Phys. Rev. E **68**, 041201 (2003).
[38] G. H. Fredrickson and H. C. Andersen, Phys. Rev. Lett. **53**, 1244 (1984).
[39] G. H. Fredrickson and H. C. Andersen, J. Chem. Phys. **83**, 5822 (1985).
[40] P. W. Anderson, in *Ill-Condensed Matter*, edited by R. Balian *et al.* (North-Holland, Amsterdam, 1979).
[41] S. Semenovskaya and A. G. Khachaturyan, Acta Mater. **45**, 4367 (1997).
[42] S. Sarkar, X. Ren, and K. Otsuka, Phys. Rev. Lett. **95**, 205702 (2005).